Elsevier Editorial System(tm) for Analytica Chimica Acta

Manuscript Draft

Manuscript Number: ACA-17-994R1

Title: Ca2+ detection utilising AlGaN/GaN transistors with ion-selective polymer membranes

Article Type: Full Length Article

Section/Category: SENSORS & BIOSELECTIVE REAGENTS

Keywords: AlGaN/GaN; chemical sensor; calcium detection; ion selective field effect transistor

Corresponding Author: Professor Giacinta Parish,

Corresponding Author's Institution:

First Author: Mohsen Asadnia

Order of Authors: Mohsen Asadnia; Matthew Myers; Gilberto A Umana-Membreno; Tarun M Sanders; Umesh K Mishra; Brett D Nener; Murray V Baker; Giacinta Parish

Manuscript Region of Origin: AUSTRALIA

***Graphical Abstract**

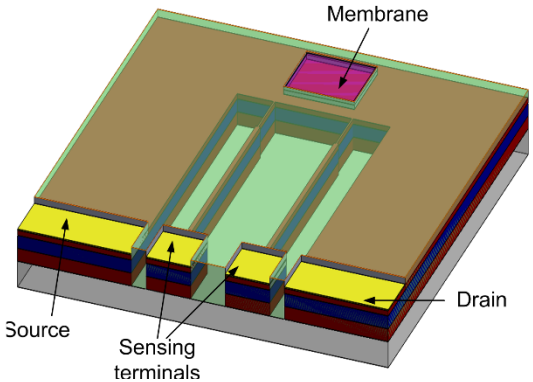

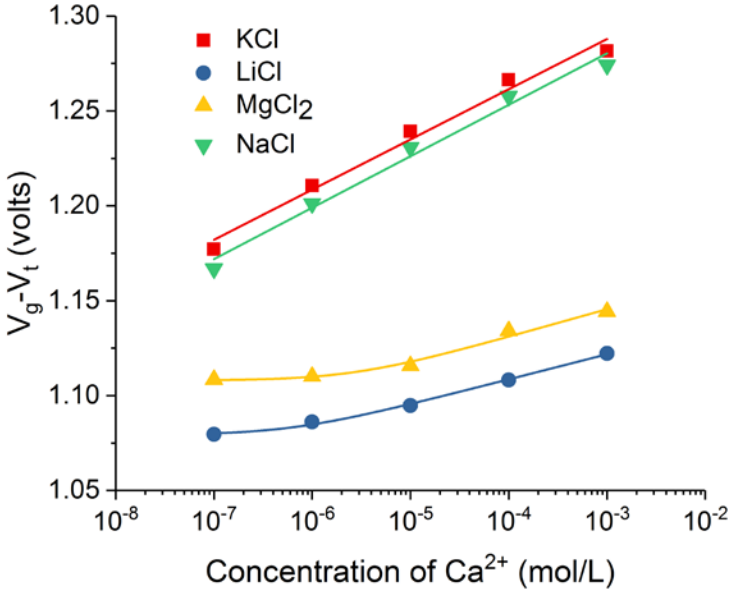

***Highlights**

Highlights

- We demonstrate reference electrode free AlGaN/GaN transistor-based Ca^{2+} sensors.
- Lower detection limit 10^{-8} M and linear response range 10^{-7}-10^{-2} M in KCl and NaCl.
- Lowest reported detection limit for reference electrode free Ca^{2+} sensors.
- Improved detection limits compared to ISEs in classical setup and previous ISFETs.
- These findings are critical for *in situ* applications of calcium ion sensing.

Ca^{2+} detection utilising AlGaN/GaN transistors with ion-selective polymer membranes

Mohsen Asadnia [a, b, *], Matthew Myers [c, d], Gilberto A. Umana-Membreno [a], Tarun M. Sanders[a], Umesh K. Mishra[e], Brett D. Nener [a], Murray V. Baker [c] and Giacinta Parish [a]

[a] School of Electrical, Electronic and Computer Engineering, The University of Western Australia, 35 Stirling Hwy., Perth, WA 6009, Australia

[b] Department of Engineering, Macquarie University, NSW 2109, Australia

[c] School of Molecular Sciences, The University of Western Australia, 35 Stirling Hwy., Perth, WA 6009, Australia

[d] CSIRO Energy Flagship, Kensington, WA 6151, Australia

[e] Department of Electrical and Computer Engineering, University of California Santa Barbara, CA 93106, USA

Abstract

We demonstrate highly selective and sensitive potentiometric ion sensors for calcium ion detection, operated without the use of a reference electrode. The sensors consist of AlGaN/GaN heterostructure-based transistor devices with chemical functionalisation of the gate area using poly (vinylchloride)-based (PVC) membranes having high selectivity towards calcium ions, Ca^{2+}. The sensors exhibited stable and rapid responses when introduced to various concentrations of Ca^{2+}. In both 0.01 M KCl and 0.01 M NaCl ionic strength buffer solutions, the sensors exhibited near Nernstian responses with detection limits of less than 10^{-7} M, and a linear response range between 10^{-7} - 10^{-2} M. Also, detection limits of less than 10^{-6} M were achieved for the sensors in both 0.01 M $MgCl_2$ and 0.01 M LiCl buffer solutions. AlGaN/GaN-based devices for Ca^{2+} detection demonstrate excellent selectivity and response range for a wide variety of applications. This work represents an important step towards multi-ion sensing using arrays of ion-selective field effect transistor (ISFET) devices.

Keywords: AlGaN/GaN; chemical sensor; calcium detection; ion selective field effect transistor

Introduction:

The detection of calcium ions, Ca^{2+}, is important in a wide range of applications. Calcium is essential for many biological functions such as neural and intracellular signalling, biomineralisation (bone, teeth), muscle action, and many enzymatic processes [1-3]. Monitoring calcium ion concentration in blood is important as deficiencies can lead to conditions such as muscle and nerve tightening [4] and osteoporosis. Water hardness can cause numerous problems in industrial processes and households, with dissolved calcium salts being the primary reason for scaling in pipes and water heaters. Further applications, where the detection of calcium ions can be crucial, include food processing [4], chemical oceanography [5] and agriculture [6, 7].

Atomic absorption spectrometry (AAS) is a traditional method often used for quantifying calcium content. However, sample preparation for AAS is tedious (acid digestion). Furthermore, AAS is often expensive, bulky and not suitable for in situ real-time monitoring. In contrast, ion selective electrodes (ISEs) have the advantages of better portability, lower cost, and excellent selectivity [8]. Furthermore, ISEs can be used for the detection of calcium in its biologically active form, Ca^{2+} [9]. Ion selective field effect transistors (ISFETs) have further advantages over traditional ISEs, such as higher signal-to-noise ratios, faster response times, and the potential for further miniaturization and integration into systems [10].

ISEs with poly(vinyl chloride) (PVC) based membranes, for the detection of Ca^{2+} ions, have demonstrated detection limits down to 5.0×10^{-7} M, linear response ranges between 8.0×10^{-7}-1.0×10^{-1} M, and stable performance over the pH range of 3.0-11.0

[10]. Similar studies using ISFETs for calcium ion detection have also reported comparable results with lower detection limits of 10^{-6} M and sensor lifetimes of up to 6 weeks [11]. The detection limits of Ca^{2+} selective ISFETs can be improved by conditioning the device in solutions containing only interfering ions to achieve zero-current ion flux for subsequent quantification of analyte solutions [12]. The type of plasticisers used in the membrane matrix can also affect the detection limit for sensors. For example, the use of *o*-nitrophenyloctyl ether (*o*-NPOE) instead of (2-ethylhexyl)sebacate (DOS) can enable detection at much lower concentrations of the analyte of interest [13]. The membranes typically consist of a polymer, a plasticiser, and neutral ion carriers (ionophores) which exhibit strong and selective binding for specific ions. Calcium ionophore ETH 1001 (or **(**(−)-(*R*,*R*)-*N*,*N*′-Bis-[11-(ethoxycarbonyl)undecyl]-*N*,*N*′,4,5-tetramethyl-3,6-dioxaoctane-diamide)) is one of these and has been widely used in clinical and biological settings for Ca^{2+} activity measurement [14, 15]. A solid-state calcium selective electrode using a poly(pyrrole) conducting polymer has the lowest reported detection limit (2.5×10^{-10} M) with linear response between 10^{-9}-10^{-4} M [16]. However, this device, like most ISEs and ISFETs, required a bulky, fragile, and a maintenance-intensive reference electrode with inner filling solution, which hinders long-term *in situ* operation.

Despite significant advances in ISEs and ISFETs, a stable reference electrode required for the long-term operation of these sensors remains elusive. Liquid junction electrodes, such as Ag/AgCl electrodes, are commonly used as reference electrodes, but suffer from electrode solution leakage that compromises the accuracy and lifetime of the sensor [17]. To date, the best results reported for a sensor operating without a reference electrode are for an ion-selective

conductometric microsensor that showed a lower detection limit of 10^{-7} M, and a dynamic range of 10^{-6}-10^{-1} M [9].

ISFETs based on AlGaN/GaN high electron mobility transistor (HEMT) devices present a compelling alternative to conventional Si-based ISFETs, with advantages such as greater chemical stability, higher device transconductance and diminished charging effects [18, 19]. The high transconductance is the result of a 2-dimensional electron gas layer (2DEG) that forms at the AlGaN/GaN interface [20]. Charges on the surface strongly influence the conductivity of the 2DEG layer, thus creating the foundation of a highly sensitive ion sensor [18, 19]. Furthermore, due to their high gain and normally-on channel, AlGaN/GaN HEMT devices do not require a reference electrode, which eliminates the associated issues of instability, bulkiness, short lifetime and drift. Previous studies have showed that AlN/GaN HEMT-based sensors can successfully measure pH in solution without the need for a reference electrode [21]. Further it has previously been demonstrated that AlGaN/GaN devices coated with appropriate functionalisation layers can detect NO_3^-, PO_4^{3-} and Hg^{2+} in solution, also without the need of a reference electrode [22-25].

We have previously reported on Ca^{2+} detection via biological mechanisms using live cells for functionalisation [26]. In this work, we report the performance of AlGaN/GaN HEMT devices functionalised by ion selective PVC-based membranes for Ca^{2+} detection. Performance characteristics of these devices such as optimal dynamic range, Nernstian slope, response time and the selectivity coefficients for a variety of interfering ions were determined.

Experimental:

Chemical materials

Calcium ionophore IV / ETH 5234 (or *N*,*N*-Dicyclohexyl-*N*′,*N*′-dioctadecyl-3-oxapentanediamide), potassium tetrakis(4-chlorophenyl)borate, 2-nitrophenyl octyl ether and high molecular weight poly(vinyl chloride) were purchased from Sigma-Aldrich and used without further purification.

Calcium selective membrane

We used the optimised formulation suggested by Gehrig et al. [27] which is 10 mg of calcium ionophore IV, 2.8 mg potassium tetrakis(4-chlorophenyl)borate, 658 mg of 2-nitrophenyl octyl ether and 329 mg of high molecular weight poly(vinyl chloride) for dissolved in 30 mL THF. A solution micro-deposition system (Vermes MDV 3200) was used to deposit a uniform layer of this material (approximately 10μm thick) onto the active area of the sensor. The sensor was then placed in a vacuum chamber overnight to remove the solvent (THF) and enhance the adhesion of the polymeric membrane to the GaN cap layer.

Device construction and operation

Figure 1 schematically represents the sensors at various stages of fabrication and packaging, prior to functionalisation by membrane deposition. The HEMT structure consists of an MOCVD-grown AlGaN/GaN structure (x_{Al} = 0.25; d_{AlGaN} = 15.5 nm) grown on a sapphire substrate. A GaN cap layer of 2 nm was also grown to improve the electrochemical stability of the device (Figure 1a). Hall effect measurements showed a carrier concentration and mobility of the HEMT sample to be 8.257×10^{12} cm^{-2} and 1472 cm^2/Vs, respectively. During fabrication the wafer was first cleaned with Technistrip (sonicating for 5 min), then rinsed with isopropanol and DI water. The wafer was then dipped into a solution of aqua regia (HNO_3:HCl=1:3) for 3 min, rinsed with DI water and blown dry with nitrogen followed by a hotplate bake for 5 min at 110°C. Standard photolithography was used for all mask patterning. Mesa

isolation was achieved using inductively coupled plasma reactive ion etching with Cl_2/Ar (see Figure 1b). The contact pads were formed by thermal evaporation of Al (200 nm), Cr (600 nm) and Au (300 nm) followed by lift-off (see Figure 1c). Rapid thermal annealing (RTA) was used to diffuse the Al through the GaN and AlGaN layers connecting (as shown in Figure 1d) the electrical contacts with the 2DEG layer at the AlGaN/GaN interface. For this step the sample was exposed to 1000 sccm N_2 in the RTA chamber at 820°C for 30 s. For device passivation, a thick layer of SU-8 (10μm) was deposited using spin-coating, and patterned using photolithography exposing only the active sensing area on the GaN cap layer (Figure 1e). Individual devices were then diced and mounted onto a pre-fabricated printed circuit board (PCB) with four electrode contacts (see Figure 1f). Conductive epoxy was used to form the connections between sensor electrodes and contacts on the PCB.

Figure 1: Schematic of the sensor at different stages of the fabrication process: (a) initial structure of GaN/AlGaN/GaN on sapphire substrate; (b) after mesa etching process to isolate individual devices; (c) after formation of contact electrodes by deposition and patterning of Al/Cr/Au metallic layers; (d) after RTA annealing to create connection between the electrodes and the 2DEG layer; (e) after SU-8 deposition and patterning for device passivation and forming the sensor active area; and (f) after mounting completed device on PCB board with four Au contact electrodes.

Figure 2a shows a schematic cross-section of the fabricated sensor with a deposited calcium sensitive membrane on the active area (see Figure 2b). The dimensions of the active area are 300 x 300 μm. Figure 2c shows an optical image of the sensor after fabrication and Figure 2d shows an optical image of the AlGaN/GaN ISFET device after packaging. During the measurements, a source-drain current of 100 μA

was maintained using a constant current circuit, whilst the sense terminals were connected to a voltage input data acquisition card (National Instruments, model 9239, 24-bit resolution). All the experiments were performed in a dark room environment to avoid the effects of light on the AlGaN/GaN device conductivity [28]. To ensure a homogenous solution and equilibrium response, the solution was stirred magnetically.

Figure 2: Device schematics showing (a) cross-section of structure and (b) 3D view of the device after fabrication, membrane deposition and SU-8 encapsulation. Optical images of the sensor (c) after fabrication and (d) after packaging onto the PCB board.

Sensor testing after functionalising the active area

After depositing the calcium sensitive membrane onto the active area of the sensor, the membrane was conditioned by immersing the device in 10^{-2} M $CaCl_2$ solution for 4 hours. The device was then removed and thoroughly rinsed with deionised water for 20 minutes. The device was then equilibrated for approximately 30 min in an ionic buffer solution of KCl without any Ca^{2+} ions. Following this initial conditioning, the device was thoroughly rinsed and soaked in de-ionised water for 20 min. For testing, the device was exposed to solutions of different interfering ions (0.01 M KCl, 0.01 M NaCl, 0.01 M $MgCl_2$ and 0.01 M LiCl) until a stable baseline was achieved (about 20-40 min). To test for different concentrations of Ca2+ against the background of interfering ions, at 30 minute intervals increasing volumes of 10^{-1} M $CaCl_2$ solution were sequentially added by pipette to achieve 10-fold increments in Ca^{2+} concentration from 10^{-8} to 10^{-2} M while continuously stirring (low speed) and monitoring the voltage at the sense terminals. The pH of the solution was not modified through the addition of acidic/basic solutions during these experiments. For

comparison the same experiments were performed with an unfunctionalized (bare gate) device.

Results and discussion

Figure 3 shows a plot of the sensor output as a function of time as Ca^{2+} was increased in 10-fold increments from approximately 10^{-8} M to 10^{-2} M in 0.01M KCl solution. The device showed a clear response to the change in Ca^{2+} ions, even at concentrations as low as 10^{-8} M. The reason for the drift and diminished response at the highest analyte concentration is unknown, but is likely due to secondary membrane effects such as Donnan exclusion failure [29]. Furthermore, the transient peaks observed in the sensor response, at the instant Ca^{2+} ion is added, may be caused by the disturbance resulting from the introduction of the additional aqueous solution, containing the ions of interest, into the measurement beaker. For the long-term and practical application of these sensors, a different methodology, such as micro-fluidics, could be used for the introduction of ionic solutions.

Figure 3: Response of GaN/AlGaN/GaN devices with calcium selective membrane to changes in Ca^{2+} concentration in a 0.01M KCl ionic buffer solution. Plot shows sensor output (voltage across sense terminals for constant forcing current of 100 μA) over a time period during which the Ca^{2+} concentration was raised from 10^{-8} M to 10^{-2} M by consecutive additions of $CaCl_2$ solution.

Figure 4 shows the sensor output vs Ca^{2+} concentration in 0.01 M KCl buffer solution for four consecutive exposure sequences at 3-day intervals. The results show minor variability and this is likely due to differing testing conditions (i.e. temperature, light exposure, etc.). Despite this, after accounting for a different offset value for each run, the sensors show a consistent response in a 0.01 M KCl solution over a period of 2 weeks, with a lower detection limit as low as 10^{-8}M in some runs (1^{st} and 3^{rd}),

and a linear response range between 10^{-7}M - 10^{-2}M, in KCl solution. The worst case (run 4) detection limit was approximately 10^{-7} M. All detection limits were determined using the IUPAC definition of detection limit for electrochemical sensors [13]. The detection limits for these sensors are, with the exception of run 4, at least one order of magnitude lower than those reported for ISFET or conventional ISE technologies as previously referenced [10, 11], and are also the best reported for reference electrode free technology [9]. While it is true that detection limits as low as 10^{-10} M have been reported for ISE technologies [13], this only occurs when the analyte concentration in the inner solution is moderated between the classical and super-Nernstian responses. However, controlling analyte concentration in an inner solution is inconvenient for on-field *in situ* operation. Finally, although not shown here, the unfunctionalised devices without PVC membrane coating showed a negligible response to Ca^{2+} ions, as expected.

Figure 4: Plot of step change ($\Delta V = V_{\text{before } Ca^{2+} \text{ added}} - V_{\text{after } Ca^{2+} \text{ added}}$) versus Ca^{2+} concentration in a 0.01 M KCl interfering ion solution for GaN/AlGaN/GaN devices with Ca^{2+} selective membrane, for four separate experiments with intervals of 4 days between each experiment. An error of approximately 3 % is determined based on three times the noise level seen in the time vs. voltage series for each set of experiments.

The method to obtain apparent changes in the applied gate voltage and ion selectivity coefficients in this work has been previously published [22, 24] and is reiterated here for the specific devices under study. Quantitative determination of the selectivity coefficients for these interfering ions requires fitting the Nikolskii-Eisenman equation to the equilibrium sensor response values; but the apparent gate voltage

change due to ion sorption into the membrane is required before this equation can be used.

The drain-source expression for field effect transistors operating in the non-saturated triode region can be described using:

$$I_D = \mu C \frac{W}{L} V_{SD} \left((V_G - V_T) - \frac{1}{2} {V_{SD}}^2 \right) \quad (1)$$

where I_D is the drain current, μ is the channel electron mobility, C is capacitance density of the gate, W is channel width, L is channel length, V_{SD} is source-drain voltage, V_G is gate voltage and V_T is threshold voltage. When drain voltages are very small ($V_{SD} \ll V_G - V_T$), Eq. (1) is approximated as:

$$I_D \approx \mu C \frac{W}{L} V_{SD} (V_G - V_T) \quad (2)$$

For this study, the current was selected to ensure operation of the device within the linear regime (triode region).

For ISFETs operated with a reference electrode, I_D and V_{SD} are maintained at constant values during sensing measurements. A feedback loop adjusts the potential applied to the reference electrode as a solution-gate for the transistor when the trans-membrane potential varies with ion concentration. This applied potential is the Nernstian response that is typically the output of an ISFET device. For our sensors, operated without a reference electrode, the device is effectively operated as a resistor and the source-drain potential, V_{SD}, is adjusted using a feedback loop to keep the drain current, I_D, constant. Changes in V_{SD}, due to exposure of the sensor to different ion concentrations, correspond to changes in channel conductivity and therefore in effective gate bias. Rearranging Eq. (2) shows that when drain current is constant (and selected for the linear regime), the conductance of the sensing layer is proportional to the gate voltage. For the particular structure used in this work (mole

fraction of x= 0.25 for the AlGaN layer and dielectric thicknesses of d_{AlGaN}=15.5nm and d_{GaN}=2nm) this relationship between change in the sensing layer conductivity and change in apparent gate voltage is given by:

$$V_G - V_T(mV) = \frac{G_{sense}(\mu S)}{0.687\ (mF/Vs)} \quad (3)$$

It should be noted that, due to electrical contact passivation with SU-8, the measured source-drain voltage (used to determine conductivity) is affected by parasitic current channels. This was not the case for the previous device design for the nitrate and mercury sensors. In this work the channel conductivity was therefore extracted from total conductivity by modelling the parasitic regions as a shunt and access resistance [30].

A linear relationship exists between the conductivity of the transistor channel and the gate voltage for the transistor device biased to operate in the linear region and hence the equilibrium response data can be represented in terms of $V_G - V_T$ by measuring the conductivity of the channel. For potentiometric sensors operated with a reference electrode, the relationship between gate voltage and potentiometric response is described by the Nikolskii-Eisenman equation:

$$V_G - V_T = E_0 - R\log\left(a_{calcium} + K \cdot {a_{ion\ buffer}}^{z_{calcium}/z_{ion\ buffer}}\right) \quad (4)$$

where E_0 is a device constant, R is potentiometric response slope, K is the selectivity coefficient, z_i the charge number and a is the activity coefficient. The expected Nernstian slope for divalent ions is $29.7\ mV$ per 10-fold change in ion concentration at room temperature. Therefore, the potentiometric response slope and the selectivity coefficients can be determined by fitting the data to Eq. 4.

Figure 5 shows the equilibrium sensor output as a function of Ca^{2+} concentration in solutions containing various interfering ions and selectivity coefficients are summarized in Table 1. These results show that Na^+ and K^+ are only weakly

interfering ions, while Mg^{2+} and Li^{+} ions affect the response much more significantly. The fitting parameters (response slope) are also given in Table 1 and show that a near-Nernstian response was obtained for KCl and NaCl. For $MgCl_2$ and LiCl, significant interference was observed and the response is sub-Nernstian. This is due to relatively stronger binding characteristics of these interfering ions with the ionophore [30]. For KCl and NaCl as interfering ions, sensor characteristics showed calcium detection limits of well below 10^{-7} M and a linear response range between 10^{-7} - 10^{-2} M. However, for $MgCl_2$ and LiCl, the detection limit increased significantly. The selectivity coefficients determined here are slightly poorer compared to values determined by Gehrig et al. using the same ionophore [27]. The reason for this might be attributed to differences in sensor design. Such limits and dynamic range are still relevant for various practical fields such as agriculture, industrial processes and biomedical applications and are the lowest detection limits reported both for ISEs in classical set-up and for any ISFET technology [10, 11], as well as for any reference electrode free operation of sensors for Ca^{2+} ions [9].

Figure 5. Plot of equilibrium sensor output represented as effective gate voltage versus Ca^{2+} ion concentration in 0.01 M KCl, NaCl, $MgCl_2$, LiCl interfering ion solutions (data points). Lines of fit show the non-linear least squares fit of this data to the Nikolskii-Eisenman equation. An error of approximately 3 % is determined based on three times the noise level seen in the time vs. voltage series for each set of experiments.

Table 1: Sensor performance in different ionic strength buffer solution. For KCl and NaCl, it is difficult to fit the data to Nikolskii-Eisenmann equation and in these cases, the estimate of the selectivity coefficient is determined based on the lower detection limit [31].

Ionic strength buffer solution	Selectivity coefficient log K	Selectivity coefficient log K (Ref.[27])	Response slope (mV/$\log_{10}[Ca^{2+}]$)	Linear response range (M)	Lower detection limit (M)
KCl	~ -3	-7.5	26.4	10^{-7}-10^{-2}	10^{-7}
NaCl	~ -3	-5.9	27.1	10^{-7}-10^{-2}	10^{-7}
$MgCl_2$	-3.6	-4.4	14.6	$10^{-5.5}$-10^{-2}	10^{-6}
LiCl	-2.2	-5.8	13.2	$10^{-5.5}$-10^{-2}	10^{-6}

Conclusion:

Detection of Ca^{2+} ions by incorporation of an ion selective membrane onto an AlGaN/GaN-based transistor device operated without the use of a reference electrode was demonstrated. For KCl and NaCl as interfering ions, sensor characteristics showed calcium detection limits of well below 10^{-7} M (10^{-8} M in the best case) and a linear response range between 10^{-7} - 10^{-2} M.

These are the lowest detection limits reported both for ISEs in classical set-up and for any ISFET technology [10, 11], as well as for any reference electrode free operation of sensors for Ca^{2+} ions [9].

Device operation without requiring a reference electrode means that associated issues of stability, maintenance and short lifetimes associated with the reference electrodes are eliminated, and opens up opportunities for miniaturisation and system integration. Despite having slightly poorer selectivity coefficients compared to previous studies using the same ionophore, it is still possible that the membrane formulation could be optimised to achieve improved selectivity. Further studies of

this technology can be expanded by integrating an array of sensors with membranes of different composition onto a single chip to detect various analytes simultaneously.

References:

[1] M.J. Berridge, M.D. Bootman, P. Lipp, Calcium - a life and death signal, Nature, 395(1998) 645-8.
[2] M.D. Bootman, T.J. Collins, C.M. Peppiatt, L.S. Prothero, L. MacKenzie, P. De Smet, et al., Calcium signalling—an overview, Seminars in Cell & Developmental Biology, 12(2001) 3-10.
[3] J.J.R.F.d. Silva, R.J.P. Williams, The biological chemistry of the elements : the inorganic chemistry of life 2nd ed. ed., New York: Oxford University Press; 2001.
[4] M.J. Lewis, The measurement and significance of ionic calcium in milk – A review, International Journal of Dairy Technology, 64(2011) 1-13.
[5] P.G. Brewer, G.T.F. Wong, M.P. Bacon, D.W. Spencer, An oceanic calcium problem?, Earth and Planetary Science Letters, 26(1975) 81-7.
[6] K.M.K. Huda, M.S.A. Banu, R. Tuteja, N. Tuteja, Global calcium transducer P-type Ca-2-ATPases open new avenues for agriculture by regulating stress signalling, Journal of Experimental Botany, 64(2013) 3099-109.
[7] G. Vardar, M. Altikatoglu, D. Ortac, M. Cemek, I. Isildak, Measuring calcium, potassium, and nitrate in plant nutrient solutions using ion-selective electrodes in hydroponic greenhouse of some vegetables, Biotechnology and Applied Biochemistry, 62(2015) 663-8.
[8] J. Bobacka, A. Ivaska, A. Lewenstam, Potentiometric ion sensors, Chem Rev, 108(2008) 329-51.
[9] U. Trebbe, M. Niggemann, K. Cammann, G.C. Fiaccabrino, M. Koudelka-Hep, S. Dzyadevich, et al., A new calcium-sensor based on ion-selective conductometric microsensors - membranes and features, Fresenius Journal of Analytical Chemistry, 371(2001) 734-9.
[10] H.A. Zamani, J. Abedini-Torghabeh, M.R. Ganjali, A highly selective and sensitive calcium(II)-selective PVC membrane based on dimethyl 1-(4-nitrobenzoyl)-8-oxo-2,8-dihydro-1H-pyrazolo 5,1-a isoindole-2,3-dic arboxylate as a novel ionophore, Bulletin of the Korean Chemical Society, 27(2006) 835-40.
[11] Y.S. K.Kao, Y. Lu, S. Gwo, J.A. Yeh, Calcium ion detection using miniaturized InN-based ion sensitive field effect transistors, International Journal of Automation and Smart Technology 2(2012) 49-54.
[12] A. Bratov, N. Abramova, C. Dominguez, Lowering the detection limit of calcium selective ISFETs with polymeric membranes, Talanta, 62(2004) 91-6.
[13] W. Bedlechowicz, M. Maj-Zurawska, T. Sokalski, A. Hulanicki, Effect of a plasticizer on the detection limit of calcium-selective electrodes, Journal of Electroanalytical Chemistry, 537(2002) 111-8.
[14] A. Bratov, N. Abramova, C. Dominguez, A. Baldi, Ion-selective field effect transistor (ISFET)-based calcium ion sensor with photocured polyurethane membrane suitable for ionised calcium determination in milk, Analytica Chimica Acta, 408(2000) 57-64.
[15] U. Schefer, D. Ammann, E. Pretsch, U. Oesch, W. Simon, Neutral carrier based Ca^{2+} selective electrode with detection limit in the sub-nanomolar range, Analytical Chemistry, 58(1986) 2282-5.
[16] A. Konopka, T. Sokalski, A. Michalska, A. Lewenstam, M. Maj-Zurawska, Factors affecting the potentiometric response of all-solid-state solvent polymeric membrane calcium-selective electrode for low-level measurements, Analytical Chemistry, 76(2004) 6410-8.
[17] H. Suzuki, T. Hirakawa, S. Sasaki, I. Karube, Micromachined liquid-junction Ag/AgCl reference electrode, Sensors and Actuators B-Chemical, 46(1998) 146-54.
[18] G. Steinhoff, O. Purrucker, M. Tanaka, M. Stutzmann, M. Eickhoff, AlxGa1-xN - A new material system for biosensors, Advanced Functional Materials, 13(2003) 841-6.
[19] B.S. Kang, H.T. Wang, F. Ren, S.J. Pearton, Electrical detection of biomaterials using AlGaN/GaN high electron mobility transistors, Journal of Applied Physics, 104(2008).

[20] O. Ambacher, B. Foutz, J. Smart, J.R. Shealy, N.G. Weimann, K. Chu, et al., Two dimensional electron gases induced by spontaneous and piezoelectric polarization in undoped and doped AlGaN/GaN heterostructures, Journal of Applied Physics, 87(2000) 334-44.
[21] A. Bengoechea Encabo, J. Howgate, M. Stutzmann, M. Eickhoff, M.A. Sanchez-Garcia, Ultrathin GaN/AlN/GaN solution-gate field effect transistor with enhanced resolution at low source-gate voltage, Sensors and Actuators B-Chemical, 142(2009) 304-7.
[22] M. Myers, F.L.M. Khir, A. Podolska, G.A. Umana-Membreno, B. Nener, M. Baker, et al., Nitrate ion detection using AlGaN/GaN heterostructure-based devices without a reference electrode, Sensors and Actuators B-Chemical, 181(2013) 301-5.
[23] K.H. Chen, H.W. Wang, B.S. Kang, C.Y. Chang, Y.L. Wang, T.P. Lele, et al., Low Hg(II) ion concentration electrical detection with AlGaN/GaN high electron mobility transistors, Sensors and Actuators B: Chemical, 134(2008) 386-9.
[24] M. Asadnia, M. Myers, N.D. Akhavan, K. O'Donnell, G.A. Umana-Membreno, U.K. Mishra, et al., Mercury(II) selective sensors based on AlGaN/GaN transistors, Analytica Chimica Acta, 943(2016) 1-7.
[25] X.L. Jia, D.J. Chen, L. Bin, H. Lu, R. Zhang, Y.D. Zheng, Highly selective and sensitive phosphate anion sensors based on AlGaN/GaN high electron mobility transistors functionalized by ion imprinted polymer, Scientific Reports, 6(2016).
[26] A. Podolska, L.C. Hool, K.D.G. Pfleger, U.K. Mishra, G. Parish, B.D. Nener, AlGaN/GaN-based biosensor for label-free detection of biological activity, Sensors and Actuators B-Chemical, 177(2013) 577-82.
[27] P. Gehrig, B. Rusterholz, W. Simon, Very lipophilic calcium. ion-selective ionophore for chemical sensors of high life-time, Chimia 43(1989) 377.
[28] J.P. Ibbetson, P.T. Fini, K.D. Ness, S.P. DenBaars, J.S. Speck, U.K. Mishra, Polarization effects, surface states, and the source of electrons in AlGaN/GaN heterostructure field effect transistors, Applied Physics Letters, 77(2000) 250-2.
[29] R.D. Johnson, L.G. Bachas, Ionophore-based ion-selective potentiometric and optical sensors, Analytical and Bioanalytical Chemistry, 376(2003) 328-41.
[30] T.M. Sanders, M. Myers, M. Asadnia, G.A. Umana-Membreno, M. Baker, N. Fowkes, et al., Description of ionophore-doped membranes with a blocked interface, Sensors and Actuators B: Chemical, 250(2017) 499-508.
[31] E. Bakker, E. Pretsch, P. Bühlmann, Selectivity of Potentiometric Ion Sensors, Analytical Chemistry, 72(2000) 1127-33.

Figure 1

Click here to download high resolution image

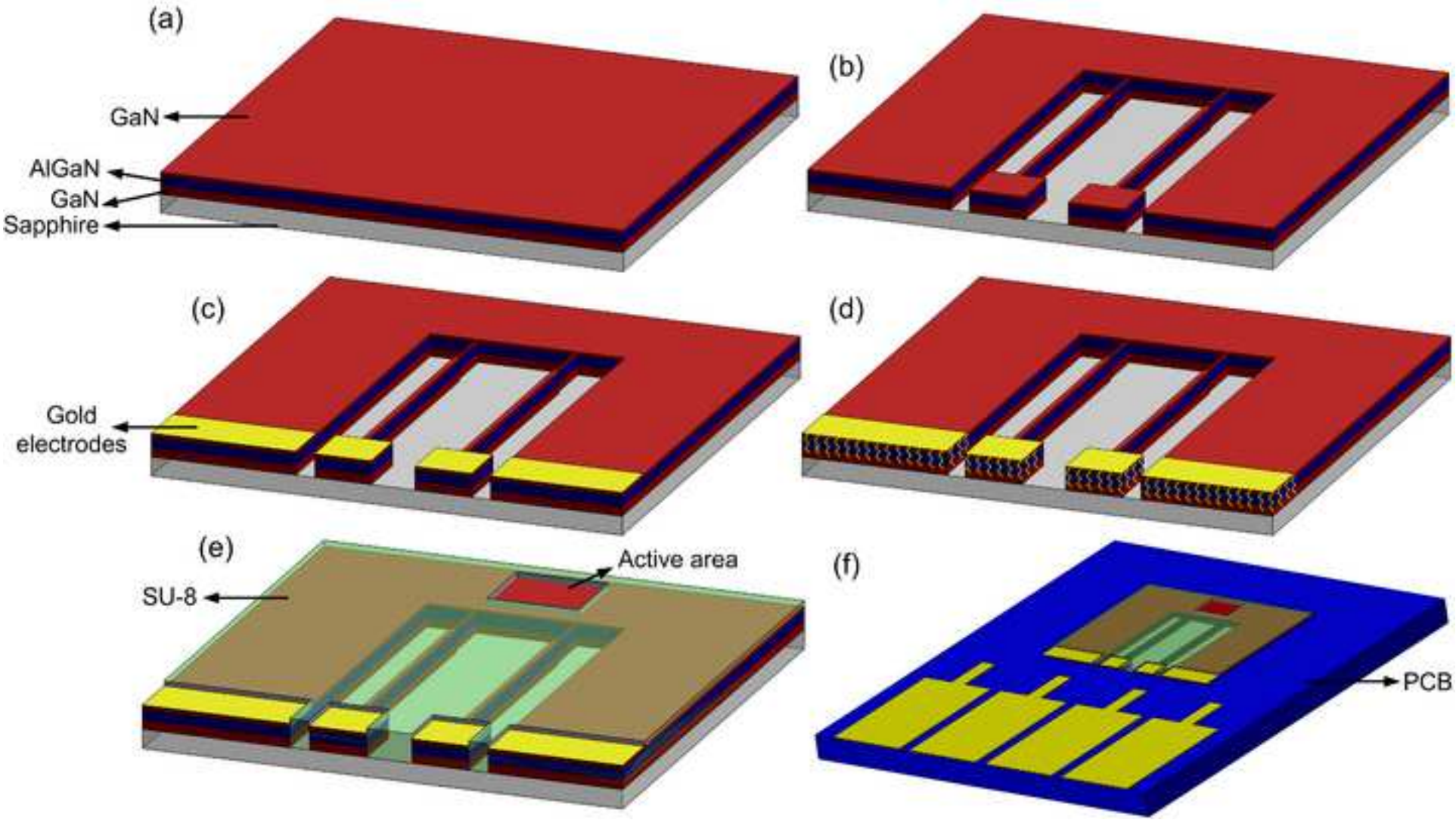

Figure 2

Click here to download high resolution image

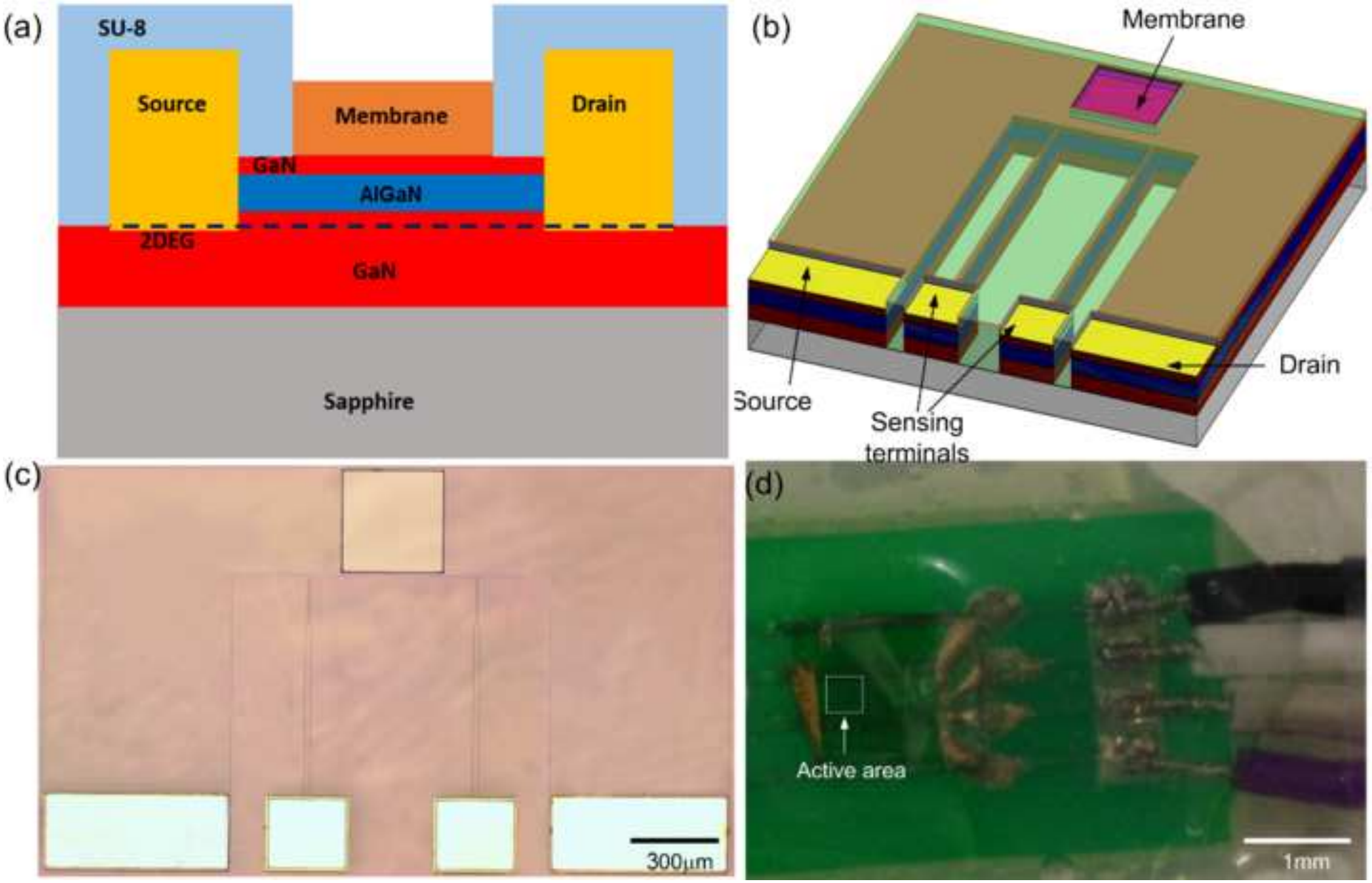

Figure 3

Click here to download high resolution image

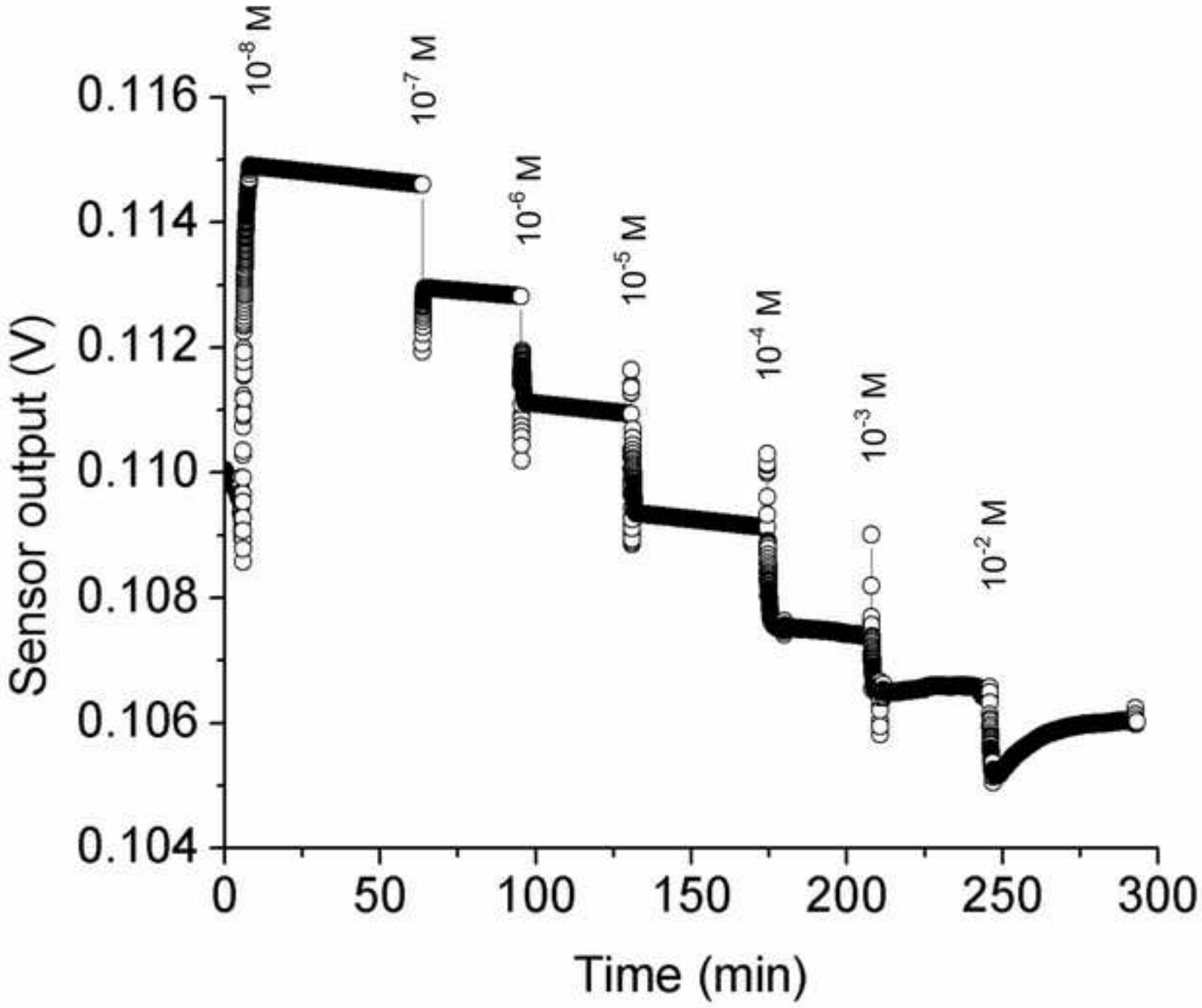

Figure 4

Click here to download high resolution image

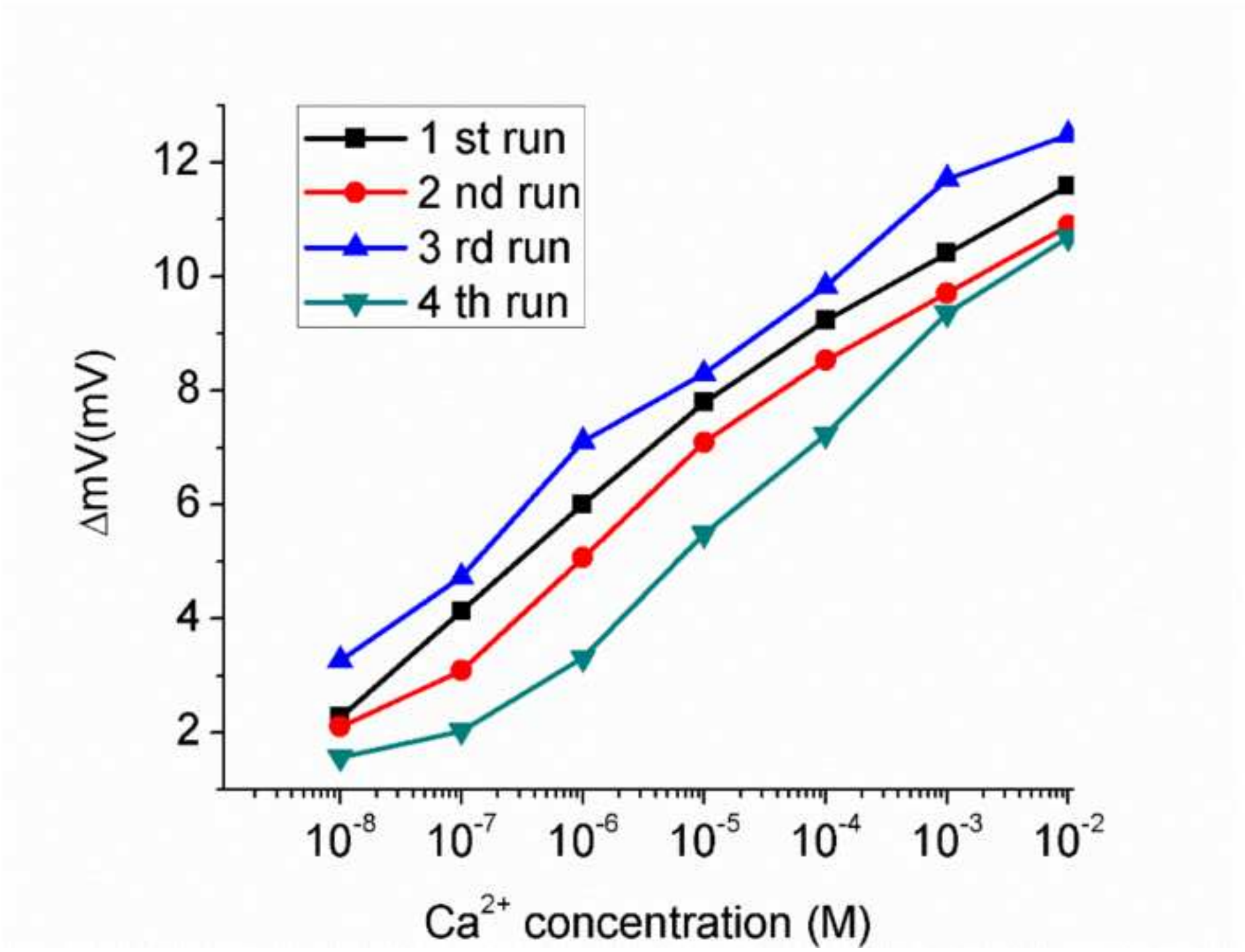

Figure 5

Click here to download high resolution image